Experimental analysis and modeling of transmission torsional vibrations

Experimental analysis and modeling of transmission torsional vibrations

ENRICO GALVAGNO*, GUIDO RICARDO GUERCIONI, MAURO VELARDOCCHIA
Department of Mechanical and Aerospace Engineering (DIMEAS)
Politecnico di Torino
C.so Duca degli Abruzzi, 24, TORINO
ITALY
http://www.polito.it/ricerca/dipartimenti/dimeas/?lang=en

Abstract: - In this article, the torsional vibrations of a transmission system installed on a test rig are investigated. The transmission system comprises a Dual Clutch Transmission (DCT) and a Manual Transmission (MT) interconnected via their output shafts. The excitation of the dynamic system is performed by two electric motors which ensure an accurate control of the speed or torque. The analysis includes the measurement of the external torques, applied by the two electric motors to the mechanical system, and the measurement of the system response in terms of angular speeds at different positions along the transmission line.
The frequency response of the system is estimated from the experimental data and compared with the simulation results of a 4-DOF lumped parameter model, which proved adequate to describe the dynamic behavior of the system up to a frequency of 100Hz.
A good match between simulation and experimental results is shown. Therefore, the model can be used to predict the torsional vibration of the transmission system under test when it behaves linearly.

Key-Words: - torsional vibrations, modal analysis, dynamic system modeling, transmission dynamics, frequency response function, experimental validation, test bench.

1 Introduction

An automotive transmission system is the path that allows the transfer of mechanical power from the prime mover of the vehicle, most frequently an internal combustion engine, to the wheels. The torque irregularity of an internal combustion engine, mainly due to the combustion process and to the inertial torque of the reciprocating masses, has a frequency spectrum that is rich in harmonic content and is related to the orders of the rotational speed.
The knowledge of the transmission transfer function matrix allows to predict the torsional vibration level of the transmission components for a given engine type and in the whole working speed and torque range. Validated torsional models of automotive transmission systems have therefore become essential tools to design and verify the vibrational behavior of a powertrain.

The torsional dynamic behavior of a Dual Mass Flywheel (DMF) is investigated in [1], both numerically and experimentally. A lumped parameter model of the torsional test rig considering two different models for the DMF damping (viscous and hysteretic) is described and experimentally validated.

In [2] the experimental and analytical methodologies for characterizing the torsional dynamic behaviour of an Automated Manual Transmission and a Dual Mass Flywheel were discussed. The effect of changing the gear ratio of the AMT in terms of compliance FRF is shown from the measures and from the simulation results of the proposed model.

In this paper after a general description of the test bench layout and functionalities, a 4-DOF torsional lumped parameter model of the whole transmission system is described. The mode shapes and natural frequencies of the modelled system are discussed and the frequency response function matrix is derived. The post processing method to estimate the frequency response functions from the experimental data will be mentioned and the comparison between simulation and experimental results will be finally presented.

(*) Corresponding Author: enrico.galvagno@polito.it

2 Transmission Test Bench

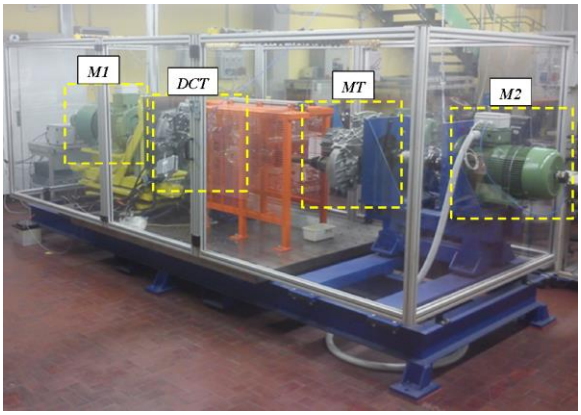

Fig. 1 - The Hardware-in-the-Loop transmission test bench at Politecnico di Torino.

Fig. 1 is a picture of the transmission test bench located in the Mechanics Laboratory at Polytechnic University of Turin (Politecnico di Torino).
It is composed mainly of the following components: two electric motors (M1 and M2) and two transmission systems for passenger car with locked differentials: a Dual Clutch Transmission (DCT) and a Manual Transmission (MT).
As can be seen from Fig. 2, both the gearboxes, DCT and MT, are used to amplify the torque delivered by the respective electric motors. The test bench connects the two motor-reducers against each other by the two output shafts, SA1 and SA2. The brake disk D is the junction point between the two electro-mechanic systems.

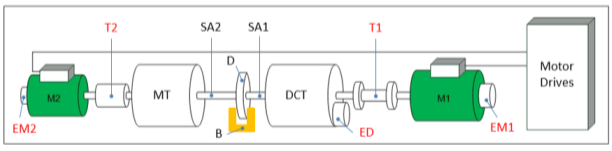

Fig. 2 – Transmission test bench layout. M1, M2: electric motors; EM1, EM2, ED: speed sensors (encoders); T1, T2: torque sensors; B: disk (D) brake; SA1, SA2: half shafts.

The test bench has many sensors, e.g. speed (encoders and inductive pick-ups), torque and temperature transducers, with the aim of monitoring the actual dynamic state of the transmission system.
Among them, during a torsional vibration test, the sensors effectively used are:

- two torque-meters, see T1 and T2 in Fig. 2, measuring the torque produced by the two electric motors;
- three incremental encoders (see Table 1 for the resolutions), EM1 and EM2 measure the angular speed of the two motors while ED measures the differential speed of the DCT that is also the output speed of the same transmission.

Encoder Location	*Pulses per revolution*
M1	1024
Diff	9000
M2	3600

Table 1 – Encoders data.

2.1 Purposes of the bench

This test bench was conceived as a Hardware-in-the-Loop test bench. It can be used to recreate manoeuvres which are representative of the real usage of a gearbox in a passenger car. This is obtained through the implementation of a simulation model running and exchanging information in real-time with the sensors and actuators of the test bench. Other examples of test benches sharing the same HiL technology are reported in [3], [4], [5].
Observing Fig. 1 from left to right there are:

- M1: a three-phase induction electric motor used to simulate the prime mover of the vehicle, e.g. the internal combustion engine;
- DCT: a 6-speed dry dual clutch transmission (see e.g. [6] for the kinematic and dynamic behaviour of this transmission);
- MT: a 6-speed manual transmission;
- M2: a second three-phase induction electric motor that simulates the vehicle load, i.e. the aerodynamic and rolling resistance, the road slope and the vehicle inertial effects.

However, Hardware-in-the-Loop tests are not the only purpose of the test bench.
The good controllability in terms of torque and speed of both the electric motors of the bench allows to generate standard (e.g. step, sine wave or chirp) or custom stimulus profiles for the excitation of the system. Moreover high resolution speed sensors along the transmission allow to accurately monitor the dynamical system response.
Also the torsional vibrations of the transmission system installed on the test bench can be investigated. On this last topic this article will be focus.

3 System modeling

The linear lumped parameter model used to study the torsional behaviour of the dynamic system is depicted in Fig. 3.

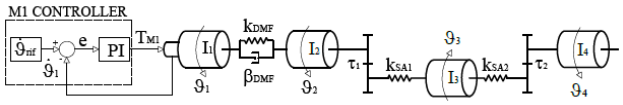

Fig. 3 – Torsional model of the test bench rotating components.

The model considers the interaction between the mechanical parts and the speed/torque controllers realized by the electric motor drives.

3.1 Electric motors control

One of the two electric motors, named M1, is speed controlled, while the second one, M2, is torque controlled. A constant speed is the setpoint for the M1 controller, while the second motor M2 applies an almost harmonic torque excitation, with a frequency which varies with time in the frequency range of interest.
The speed control of the electric motor M1 is implemented as a Proportional Integrative (PI) controller:

$$T_{M1} = k_P\left(\dot{\theta}_{rif} - \dot{\theta}_{M1}\right) + k_I \int (\dot{\theta}_{rif} - \dot{\theta}_{M1})dt \qquad (1)$$

being k_P and k_I the proportional and integrative gains respectively.
Eq.1 can be rearranged as follows:

$$T_{M1} = k_P \cdot \dot{\theta}_{rif} + k_I \int \dot{\theta}_{rif} dt - k_P \cdot \dot{\theta}_{M1} - k_I \int \dot{\theta}_{M1} dt \qquad (2)$$

Under the assumption that the speed set-point is constant ($\dot{\theta}_{rif} = cost$), the former equation is further simplified:

$$T_{M1} = \dot{\theta}_{rif} \cdot (k_P + k_I \cdot t) - k_I \cdot \theta_{M1} - k_P \cdot \dot{\theta}_{M1} \qquad (3)$$

Eq. (3) shows that the integral gain acts as a torsional stiffness, i.e. the elastic term is $k_I \theta_{M1}$, and the proportional gain as a viscous damping, the viscous term is $k_P \dot{\theta}_{M1}$, which connect the first inertia of the system to the ground.
The torque applied by electric motor M2 is a different matter. In fact, considering small oscillations around an equilibrium point and neglecting the constant torque that the motors have to deliver to guarantee that steady-state condition, it is not necessary to make explicit the torque applied by the electric motor M2. An harmonic excitation applied to one of the inertias of the system, the one having moment of inertia I_4 in this case, is implicit in the receptance method [6].

3.2 Torsional system dynamics

A 4-DOF torsional system is used to describe the dynamic behaviour of the mechanical system under test.
The two gearboxes are modelled as simple gear pairs characterised by the actual gear ratio τ_1 and τ_2, defined as the quotient between input and output speed, and unitary efficiency.
Also the Dual Mass Flywheel of the DCT is installed on the test bed, therefore a low stiffness k_{DMF} spring and a high damping β_{DMF} viscous damper are introduced in the model. The moment of inertia of the first DMF mass is added to the M1 rotor inertia just before the spring and damper element, while the second mass is added to the equivalent inertia of the DCT evaluated at its input shaft. The two half shafts SA1 and SA2 are modelled as purely elastic elements.
The generalized coordinates are the angular position of each flywheel composing the system: $q = \{\theta_1\ \theta_2\ \theta_3\ \theta_4\}^T$.

The equation of motions of the torsional system depicted in Fig. 3 are:

$$\begin{cases} I_1 \cdot \ddot{\theta}_1 + k_{DMF} \cdot (\theta_1 - \theta_2) + \beta_{DMF} \cdot (\dot{\theta}_1 - \dot{\theta}_2) + \beta_1 \cdot \dot{\theta}_1 + T_{M1} = 0 \\ I_2 \cdot \ddot{\theta}_2 + \beta_2 \cdot \dot{\theta}_2 - k_{DMF} \cdot (\theta_1 - \theta_2) - \beta_{DMF} \cdot (\dot{\theta}_1 - \dot{\theta}_2) - \frac{k_{SA1}}{\tau_1} \cdot \left(\theta_3 - \frac{\theta_2}{\tau_1}\right) = 0 \\ I_3 \cdot \ddot{\theta}_3 + \beta_3 \cdot \dot{\theta}_3 + k_{SA1} \cdot \left(\theta_3 - \frac{\theta_2}{\tau_1}\right) + k_{SA2} \cdot \left(\theta_3 - \frac{\theta_4}{\tau_2}\right) = 0 \\ I_4 \cdot \ddot{\theta}_4 + \beta_4 \cdot \dot{\theta}_4 - \frac{k_{SA2}}{\tau_2} \cdot \left(\theta_3 - \frac{\theta_4}{\tau_2}\right) = 0 \end{cases} \qquad (4)$$

The system of equation can be cast in matrix form:

$$[M]\{\ddot{q}\} + [B]\{\dot{q}\} + [K]\{q\} = \begin{Bmatrix} 1 \\ 0 \\ 0 \\ 0 \end{Bmatrix} \dot{\theta}_{rif,M1}(k_P + k_I t) \qquad (5)$$

where the mass, damping and stiffness matrices are respectively:

$$[M] = \begin{bmatrix} I_1 & 0 & 0 & 0 \\ 0 & I_2 & 0 & 0 \\ 0 & 0 & I_3 & 0 \\ 0 & 0 & 0 & I_4 \end{bmatrix}$$

$$[\mathrm{B}] = \begin{bmatrix} \beta_{DMF} + \beta_1 + k_P & -\beta_{DMF} & 0 & 0 \\ -\beta_{DMF} & \beta_{DMF} + \beta_2 & 0 & 0 \\ 0 & 0 & \beta_3 & 0 \\ 0 & 0 & 0 & \beta_4 \end{bmatrix}$$

$$[K] = \begin{bmatrix} k_{DMF} + k_I & -k_{DMF} & 0 & 0 \\ -k_{DMF} & k_{DMF} + \frac{k_{SA1}}{\tau_1^2} & -\frac{k_{SA1}}{\tau_1} & 0 \\ 0 & -\frac{k_{SA1}}{\tau_1} & k_{SA1} + k_{SA2} & -\frac{k_{SA2}}{\tau_2} \\ 0 & 0 & -\frac{k_{SA2}}{\tau_2} & \frac{k_{SA2}}{\tau_2^2} \end{bmatrix} \quad (6)$$

Note that the proportional gain k_P appears in the damping matrix, while the integral gain k_I in the stiffness matrix.

3.3 Natural frequencies and mode shapes

By solving the eigenvalue problem associated with the undamped system, i.e.

$$([K] - \omega_i{}^2[M])\{\psi\}_i = \{0\}, \quad i = 1,2,3,4 \quad (7)$$

you get the natural frequencies $f_i = \frac{\omega_i}{2\pi}$ and the associated mode shapes, described by the natural modes or modal vectors $\{\psi\}_i$.

The mode shapes were normalized with the aim of having the modulus of the maximum element of each eigenvector equal to one.

Moreover, due to the presence of two gear ratios, i.e. the transmission ratio of the two gearboxes, along the transmission line it is convenient to show the eigenvectors referred to the same shaft, e.g. the shaft of the electric motor M1. As an example the *r-th* eigenvector is scaled as follows:

$$\{\psi\}_{r,M1} = \left\{ \psi_1 , \psi_2 , \tau_1\psi_3 , \frac{\tau_1}{\tau_2}\psi_4 \right\}_r^T \quad (8)$$

Fig. 4 shows the natural frequency and the mode shape referred to M1 shaft for each of the four vibration modes.

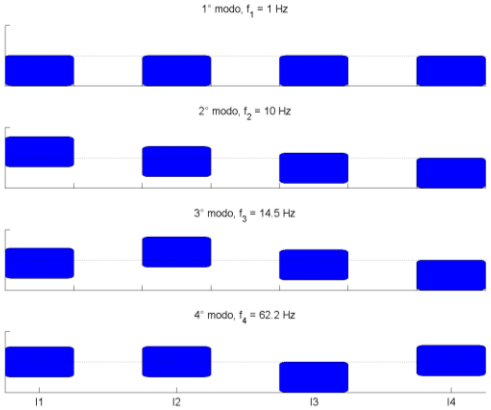

Fig. 4 – Natural frequencies and mode shapes computed from the simulation model.

The first low frequency (≈1 Hz) mode, is almost a rigid body mode and it is primarily associated with the electric motor speed controller. The increase in the integral gain k_I of the PI controller determines an increase of the first resonance frequency of the system, while the proportional gain k_P increases the damping factor relating to this mode.

The second mode is the first real torsional mode of the system. The 2nd and 3rd natural frequencies are very close to each other (10Hz the second, 14.5Hz the third), hence their individual effects combine to give rise to a single peak in the frequency response at an intermediate frequency between the two, i.e. 12.5 Hz. The inertia of the electric motor M1 (I_1) reduces that frequency, while the increase of the second flywheel mass (I_2) amplifies the peak amplitude. The half-shafts stiffness moves the peak to higher frequencies. If the DMF damping is small enough there are two separate peaks; the increase of damping initially flatten the two peaks and then produces an increase of the single peak amplitude.

The 4th mode is due to the vibration of the brake disk I_3 with respect to the remaining part of the driveline that remains practically stationary. The dynamic behaviour of the system and its sensitivity to the parameters in the neighbourhood of the highest natural frequency is similar to that of a 1-DOF system having inertia I_3, stiffness $k_{SA1} + k_{SA2}$ and damping β_3.

3.4 Frequency response functions

The response of a viscously damped n-DOF system to harmonic external excitation can be calculated by means of the receptance matrix $\alpha(\Omega)$, relating the displacement of each degree of freedom θ to the excitation T as a function of frequency:

$$\{\theta_0\} = [\alpha(\Omega)]\{T_0\} \quad (9)$$

where $\{T_0\}$ is a real vector of constant amplitudes while $\{\theta_0\}$ is a complex vector. The matrix $\alpha(\Omega)$ can be calculated as the inverse of the dynamic stiffness matrix:

$$[\alpha(\Omega)] = [K_{dyn}]^{-1} = ([K] + j\Omega[B] - \Omega^2[M])^{-1} \quad (10)$$

The measures on the test bench are angular speeds and torques, hence the FRFs we want to extract from the model are the ratios between these two quantities, called "mobility functions".

Under harmonic regime of motion the relationship between speed and angular position amplitudes is:

$$\dot{\theta}_0 = \mathrm{j}\,\Omega\,\theta_0 \quad (11)$$

Inserting eq. (9) into eq. (11), we obtain:

$$\{\dot{\theta}_0\} = \mathrm{j}\,\Omega\,[\alpha(\Omega)]\{T_0\} \tag{12}$$

More specifically, since the harmonic torque is applied from electric motor M2 to the 4th inertia of the system, i.e. the unique element of $\{T_0\}$ different from zero is the fourth one ($\{T_0\} = \{0\ 0\ 0\ 1\}^T \cdot T_0$), the set of equations representing the frequency response of each degree of freedom contains only the fourth column of the receptance matrix:

$$\begin{Bmatrix} \dot{\theta}_{M1} \\ \dot{\theta}_2 \\ \dot{\theta}_3 \\ \dot{\theta}_{M2} \end{Bmatrix} / T_{M2} = \mathrm{j}\Omega \begin{Bmatrix} \alpha_{1,4}(\Omega) \\ \alpha_{2,4}(\Omega) \\ \alpha_{3,4}(\Omega) \\ \alpha_{4,4}(\Omega) \end{Bmatrix} \tag{13}$$

4 Experimental tests

During a torsional vibration test, while one electric motor, the torsional exciter system, produces a sinusoidal torque having constant amplitude and continuously variable frequency (torque control is enabled for this motor), the second one tries to keep constant the speed of its shaft (closed-loop speed control mode enabled). By doing so the system under test is excited in the whole frequency range of interest.

It should be noted that, before the torsional excitation starts, the system must be brought to a steady state condition, i.e. constant speed and torque, where the behaviour of the system can be linearized. A torque offset must be therefore constantly applied and added to the harmonic trend during the test, in order to have: approximately constant system parameters, e.g. no appreciable stiffness variations, and no crossing of the line of zero torque to avoid the nonlinear phenomena associated with load reversal (impact between the rotating component due to backlash).

Time histories of the torques applied by the two electric motors are measured and collected together with the angular speeds in three points of the transmission line.

A post processing tool based on the H_2 estimator, see e.g. [8] and [2] for details, applied to the acquired data gives the transfer functions between the input torque, applied by the electric motor that excites the system, and the rotational speeds.

Even if an external load is applied by both the electric motors, a single-input multiple-output (SIMO) approach can be used to analyse the dynamic behaviour of the system. The close-loop speed controller of the electric motor must become part of the system under test and so its mathematical description was included in the model.

Fig. 5-Fig. 8 show the FRFs estimated from the measures. Since the excitation for the dynamic system is generated by the electric motor M2, the amplitude of the response $\dot{\theta}_{M2}$ is high enough to be measured accurately by the encoder up to 100 Hz. Conversely, the lower amplitude of oscillation of the other electric motor M1 considering also the lower sensor resolution, limit the range of reliability of $\dot{\theta}_{M1}/T_{M2}$ to 20 Hz.

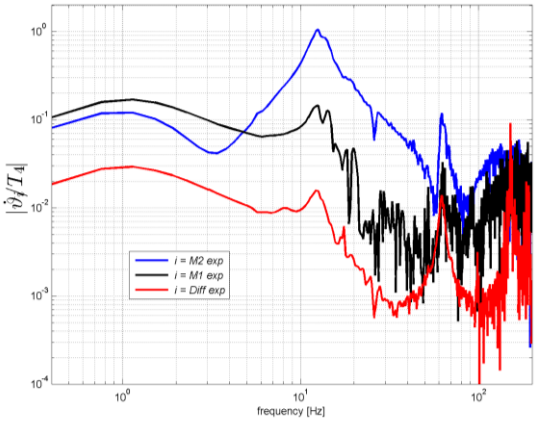

Fig. 5- Magnitude of the FRFs estimated from experimental data.

The sensors used to measure the angular velocity of the three instrumented shaft are incremental encoders having different resolutions as shown in Table 1. High resolution encoders allow to push the frequency analysis towards higher frequencies. As an example, even if the amplitude of the oscillation at the differential output is the lowest (see Fig. 5), the FRF shows a clear trend up to more than 100Hz, as also confirmed by the coherence function shown in Fig. 8.

A resonance peak at a frequency higher than 100 Hz is visible in the differential FRF, but it cannot be captured by the current model. In fact a 4-DOF model can give rise to at most 4 resonance peaks. In this specific case two of them are very close therefore producing a unique peak. An extra DOF should be added to the system model to catch the aforementioned resonance peak. The frequency range of analysis is coherently limited to 100 Hz.

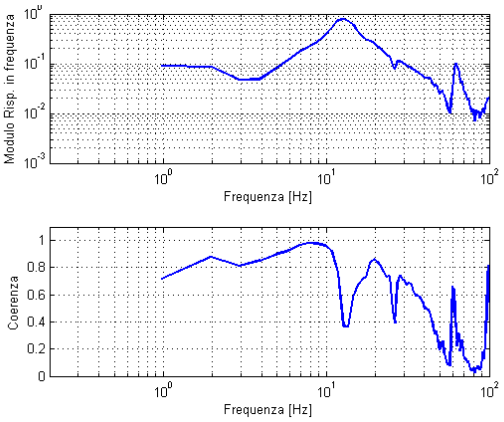

Fig. 6 – FRF $\dot{\theta}_{M2}/T_{M2}$: modulus (top) and coherence function (bottom).

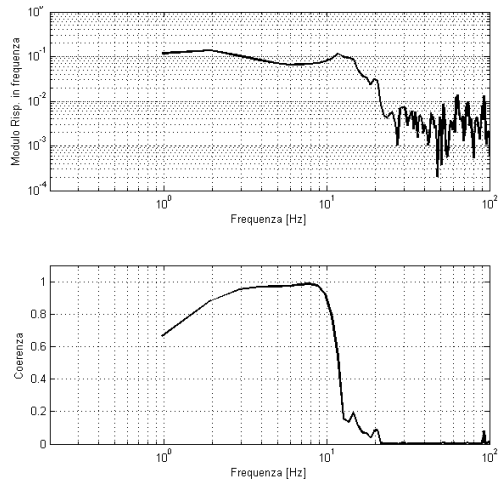

Fig. 7 - FRF $\dot{\theta}_{M1}/T_{M2}$: modulus (top) and coherence function (bottom).

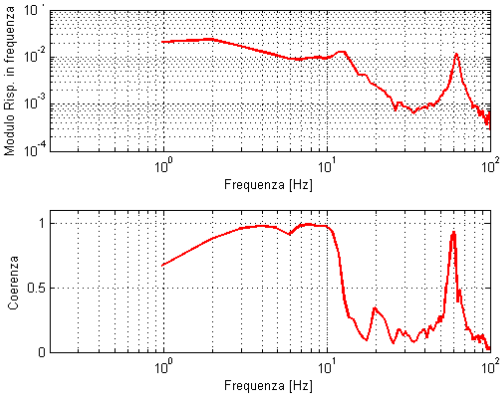

Fig. 8 – FRF $\dot{\theta}_{Diff}/T_{M2}$: modulus (top) and coherence function (bottom).

5 Model validation

In this section a comparison between the model results and the experimental data is shown.

The plots reported in Fig. 9 and Fig. 10 represent the simulated FRF, calculated numerically by evaluating eq. (13), and the estimated FRF using the measures of torque and speed from the test rig.

A very good match between the experimental an simulated curves can be seen in Fig. 9, in the whole frequency range, and in Fig. 10, at least up to the limit of reliability of the experimental data (20 Hz). The frequency and amplitude of the resonance peaks are well captured by the model.

Further parameter tuning, especially in terms of damping could increase the accuracy of the phase curve. Also different damping model, such as the hysteretic one could be test at least for the DMF [1].

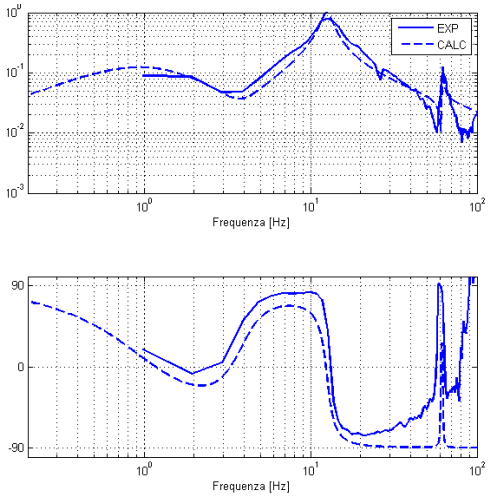

Fig. 9 – FRF of $\dot{\theta}_{M2}/T_{M2}$: modulus (top), phase [°] (bottom)

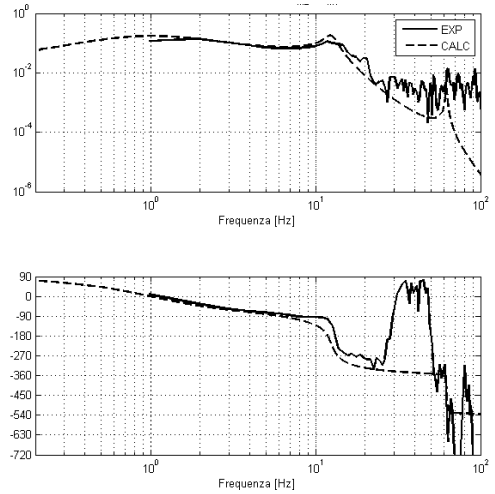

Fig. 10 - FRF $\dot{\theta}_{M1}/T_{M2}$: modulus (top) and phase [°] (bottom).

6 Conclusion

In this paper the torsional vibrations of a transmission system mounted on a test rig were investigated. The system under test is composed of a dual clutch transmission and a manual transmission and is loaded by two induction electric motors.

The 4-DOF lumped parameter model presented in the paper has proved suitable to describe the transmission vibrations up to a maximum frequency of 100 Hz. A good match between the experimental an simulated FRF curves is shown, at least up to the limit of reliability of the experimental data.

The first highly damped torsional mode of the transmission system (≈1 Hz) is almost a rigid body mode and it is primarily associated with the electric motor speed controller.

The second mode is the first real torsional mode of the system. The 2nd and 3rd natural frequencies are very close to each other, hence their individual effects combine to give rise to a single peak in the FRFs at about 12.5 Hz.

The 4th mode represents the vibration of the brake disk with respect to the remaining part of the driveline that remains practically stationary.

References:

[1] Galvagno, E., Velardocchia, M., Vigliani, A. and Tota, A., Experimental Analysis and Model Validation of a Dual Mass Flywheel for Passenger Cars, *SAE Technical Paper Nr. 2015-01-1121, SAE Word Congress 2015*, Detroit (MI), USA, April 21-23, 2015, pp. 1-8.

[2] Galvagno, E., Tota, A., Velardocchia M., and Vigliani, A., Test Bench Characterisation and Frequency Domain Torsional Model Validation of Transmission Systems and Components, *TrC-IFToMM Symposium on Theory of Machines and Mechanisms*, Izmir, Turkey, June 14-17, 2015, pp.1-9.

[3] Mendes, A. and Meirelles P., Application of the Hardware-in-the-Loop Technique to an Elastomeric Torsional Vibration Damper, *SAE Int. J. Engines*, Vol.6, No.4, 2013, pp. 2004-2014.

[4] Sorniotti, A., D'Alfio, N., Galvagno, E., Morgando, A. & Amisano, F., Hardware-In-the-Loop Testing of Automotive Control Systems, *SAE Technical Paper Nr. 2006-01-1962*, 2006, pp. 1-14.

[5] Bracco, G., Giorcelli, E., Mattiazzo, G., Orlando, V., and Raffero, M. (2014). Hardware-In-the-Loop test rig for the ISWEC wave energy system, *Mechatronics*, Vol.25, 2015, pp.11-17, doi:10.1016/j.mechatronics.2014.10.007.

[6] Galvagno E., Velardocchia M., Vigliani A., Dynamic and kinematic model of a dual clutch transmission, *Mechanism and Machine Theory*, Vol. 46, No. 6, pp. 794-805. - ISSN 0094-114X.

[7] Meirovitch, L., *Fundamentals of Vibrations*, McGrawHill, International Edition 2001.

[8] Brandt, A., *Noise and Vibration Analysis - Signal Analysis and Experimental Procedures*, John Wiley & Sons, Ltd., 2010, ISBN: 978-0-470-74644-8.

Definitions/Abbreviations/Symbols

B	Brake
D	Brake Disk
DCT	Dual Clutch Transmission
DOF	Degree of Freedom
Diff	DCT Differential
DMF	Dual Mass Flywheel
E	Encoder
FRF	Frequency Response Function
HiL	Hardware-in-the-Loop
M1/M2	Electric Motors
MT	Manual Transmission
SA1/SA2	Half shafts
k	Torsional stiffness
j	Imaginary unit
β	Viscous damping coefficient
$\theta, \dot{\theta}, \ddot{\theta}$	Angular position, speed and acceleration
τ_1	Gear ratio ($\dot{\theta}_{in}/\dot{\theta}_{out}$) of the DCT
τ_2	Gear ratio of the MT
Ω	Angular frequency
I	Mass moment of inertia
T	Torque
T1/T2	Torque sensors
$[\alpha]$	Receptance matrix
$[B]$	Damping matrix
$[K]$	Stiffness matrix
$[M]$	Mass matrix
$\{\psi\}_i$	Natural mode *i*
ω_i	Natural frequency of *i-th* mode